Toward Highly Sensitive Polymer Photodetectors by Molecular Engineering

Luozheng Zhang, Tingbin Yang, Liang Shen, Yanjun Fang, Li Dang, Nanjia Zhou, Xugang Guo, Ziruo Hong, Yang Yang, Hongbin Wu, Jinsong Huang,* and Yongye Liang**

Owing to their potential advantages over inorganic semiconductors, conjugated polymers have attracted broad interest from academy and industry for optoelectronic applications.[1–3] Their solution processability could offer the potential of simple processing and low-cost fabrication of the semiconductor devices.[4–6] Besides, conjugated polymers also possess the advantages of mechanical flexibility, light weight, semitransparency, and tunability of optoelectrical properties by structural engineering, which could facilitate novel applications of optoelectronics.[7,8] Successful applications of conjugated polymers have been demonstrated in photovoltaics,[9,10] field-effect transistors,[11,12] and light-emitting diodes.[13,14]

Conjugated polymers can also be applied as active materials for photodetectors, which is important for environmental monitoring, data communication, image sensing, and so on.[15–18] High external efficiency, fast response, and selective or broad detection from ultraviolet (UV) to near infrared (NIR) range have been demonstrated in polymer photodetectors.[19,20] Besides, they are suitable for large area detection and could be operated at room temperature and on flexible substrates, affording new opportunities for sensing and detecting technologies.[21] Similar to polymer solar cells, bulk heterojunction structure is often employed to construct polymer photodetectors, with conjugated polymer as the electron donor and fullerene derivative as the electron acceptor.[9,22] It favors photon absorption and charge separation, affording high external quantum efficiency and responsivity. However, polymer photodetectors with bulk heterojunction structure usually suffer a relatively high dark current density (J_d) at negative bias and low rectification ratio between forward/reverse bias due to unfavorable charge transport and injection. For example, Cao and co-workers developed a poly[5,7-bis(4-decanyl-2-thienyl)thieno[3,4-b]diathiazole-thiophene-2,5] (PDDTT) based photodetector with response to 1220 nm. In a normal device structure of indium tin oxide/poly(3,4-ethylenedioxythiophene):poly(styrenesulfonate)/PDDTT:$PC_{61}BM$/Ba/Al,(ITO/PEDOT:PSS/PDDTT:$PC_{61}BM$/Ba/Al), it showed a J_d of about 1×10^{-5} A cm^{-2} at –2 V.[23] The PTT photodetector developed by Yu and Yang et al. also exhibited a J_d around 1×10^{-5} A cm^{-2} at –2 V.[24] Since the shot noise coming from dark current plays a dominant role in the electronic noise, the high J_d at negative bias lowers the signal/noise ratio, limiting the detectivity of polymer photodetectors.[25]

Previous works to overcome the dark current problem are generally confined to interface modification, morphology control, and thickening the active-layer, especially to the first case.[25] Gong et al. improved the performance of PDDTT-based photodetectors by modifying the multi-interfacial layers between the active layer and the electrodes. The device structure was ITO/PEDOT:PSS/polystyrene-N,N-diphenyl-N,N-bis(4-n-butylphenyl)-(1,10-biphenyl)-4,4-diamine-perfluorocyclobutane (PS-TPD-PFCB)/PDDTT:$PC_{61}BM$/C_{60}/Al), which could effectively reduce the dark current of the devices to 1×10^{-9} A cm^{-2} biased at –0.1 V. As a result, the photodetector exhibited photodetectivity greater than 10^{12} Jones (1 Jones = 1 cm Hz$^{1/2}$ W^{-1}) from 1150 to 1450 nm.[19] Verilhac and co-workers introduced polyethylenimine (PEIE) to modify the cathode in an inverted structure. The thin PEIE layer could lower the work function of the cathode, leading to a low J_d of 2×10^{-9} A cm^{-2} at –2 V bias by depressing unexpected hole injection from the cathode.[26] Gong et al. further demonstrated that the leakage currents of the NIR polymer photodetectors can be prevented by the employment of wide bandgap quantum dots.[27] However, these methods required complicate processing and could be difficult to be applied in other systems. Also, the reported methods to reduce dark current usually led to significant decrease of charge transport/injection, which could affect other parameters of photodetectors.[26,28–30]

Dr. L. Z. Zhang, Dr. T. B. Yang,
Prof. X. G. Guo, Prof. Y. Y. Liang
Department of Materials Science and Engineering
South University of Science and Technology of China
Shenzhen 518055, P. R. China
E-mail: liang.yy@sustc.edu.cn
Dr. L. Shen, Dr. Y. Fang, Prof. J. Huang
Department of Mechanical and Materials Engineering
University of Nebraska-Lincoln
Lincoln, NE 68588, USA
E-mail: jhuang2@unl.edu
Prof. L. Dang
Department of Chemistry
South University of Science and Technology of China
Shenzhen 518055, P. R. China
Dr. N. J. Zhou
Department of Chemistry and the Materials Research Center
the Argonne-Northwestern Solar Energy Research Center
Northwestern University
2145 Sheridan Road, Evanston, IL 60208, USA
Dr. Z. Hong, Prof. Y. Yang
Department of Materials Science and Engineering
University of California
Los Angeles, CA 90095, USA
Prof. H. B. Wu
State Key Laboratory of Luminescent Materials and Devices
South China University of Technology
Guangzhou 510640, P. R. China
E-mail: hbwu@scut.edu.cn

DOI: 10.1002/adma.201502267

Herein, we introduce a new approach to develop efficient polymers for photodetector application with high sensitivity by modifying the polymer structures with 3,4-ethylenedioxythiophene (EDOT) side chains conjugated to the semiconducting polymer backbone. The introduction of EDOT effectively lowers the J_d of the photodetector device by about two orders of magnitude with little decrease in the external quantum efficiency (EQE) compared with the control device made of polymer without EDOT side chains. Thus, the photodectivity could increase by more than one order of magnitude. This approach can be applied to a variety of semiconducting polymers with photoresponse covering from UV to NIR, which can provide a general and feasible way to fabricate efficient polymer photodetectors with high photodetectivity.

Benzo[1,2-*b*:4,5-*b*′]dithiophene (BDT) was employed as a model building block to construct the polymers, as its extended conjugation, high planarity, and small steric hindrance with adjacent units are beneficial for high photovoltaic performance.[8,31] To tune the properties of BDT, alkyl (such as 2-ethylhexyl chain) substituted 3,4-ethylenedioxythiophene was introduced to the 4, 8 positions as side chains. The polymers were easily accessed by Stille poly-condensation reaction between the bis-stannylated BDT-based donor units and various dibrominated acceptor units. Thieno[3,4-*c*]pyrrole-4,6-dione (TPD) and diketopyrrolopyrrole (DPP) were chosen as acceptor units because of the good photovoltaic performance of their polymers.[32,33] **Scheme 1** shows the molecular structures of the polymers (electron donors), [6,6]-phenyl C_{61}-butyric acid methyl ester ($PC_{61}BM$), and [6,6]-phenyl C_{71}-butyric acid methyl ester ($PC_{71}BM$) (electron acceptors).

To investigate the effect of EDOT unit on the optical properties of the polymers, the absorption data in solid films (**Figure 1**a) and solutions (Supporting Information, Figure S1) were measured. In general, the EDOT-modified polymers exhibited similar absorption spectra to the control polymers with thiophene as side chains. For TPD polymer films, EDOT polymer showed a higher ratio of peak absorption (608 nm) to shoulder absorption (553 nm) compared with thiophene modified one. DPP polymers also exhibited a similar trend. It is possibly related to the enhanced intramolecular interaction after the introduction of electron donating EDOT chains. The absorption spectra of EDOT polymers showed blue shifts compared with their thiophene counterparts, especially in TPD polymers. It suggested that the bulkier EDOT chain could cause a larger conformational distortion of the conjugated backbone, increasing the bandgap. The energy levels of the polymers were measured by cyclic voltammetry (CV) (Supporting Information, Figure S2). The highest occupied molecular orbital (HOMO) and the lowest unoccupied molecular orbital (LUMO) of the polymers are shown in Figure 1b. As the EDOT unit is more electron-donating than thiophene, EDOT polymers exhibited slightly higher HOMO energy levels compared with the thiophene polymers. The introduction of EDOT caused a slight increase of the polymer bandgap compared with thiophene polymer, in consistence with the absorption data. The molecular simulations by density functional theory (DFT) revealed similar changes as observed from absorption and CV data (Supporting Information, Figure S3).

In order to evaluate the optoelectronic properties, photodetectors based on these polymers were fabricated. The device structure is shown in **Scheme 2**. The device consisted of a substrate of indium tin oxide (ITO) modified with a layer of poly(3,4-ethylenedioxythiophene):poly(styrenesulfonate) (PEDOT:PSS) as an anode, a conjugated polyelectrolyte poly[(9,9-bis(3′-(*N*,*N*-dimethylamino)propyl)-2,7-fluorene)-*alt*-

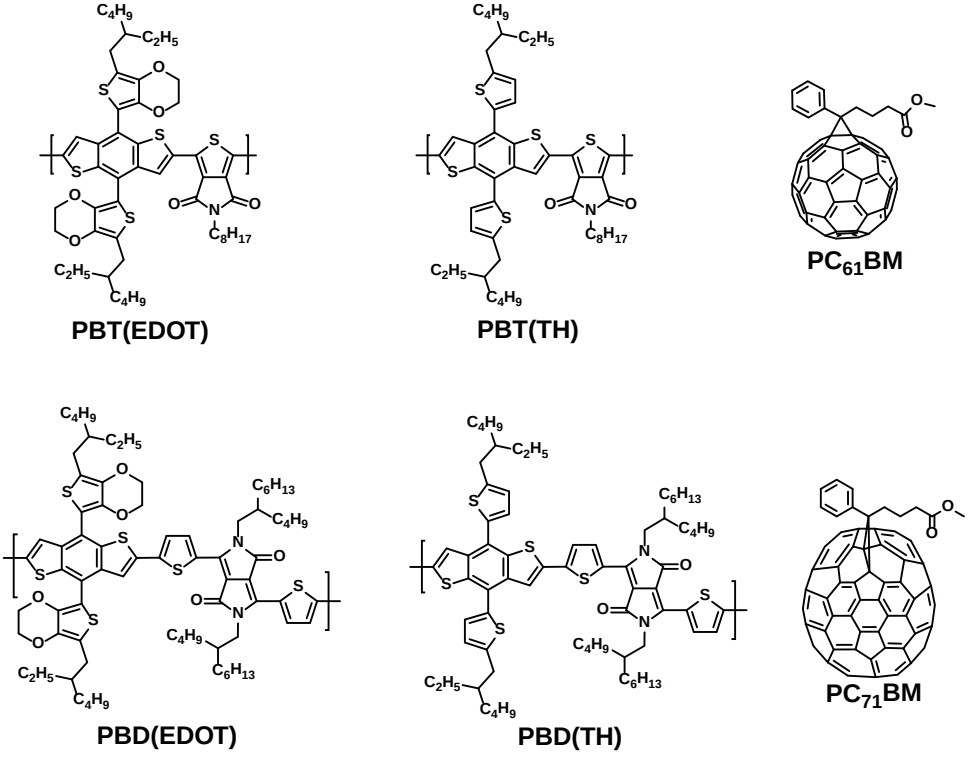

Scheme 1. The molecular structures of the electron donors and acceptors.

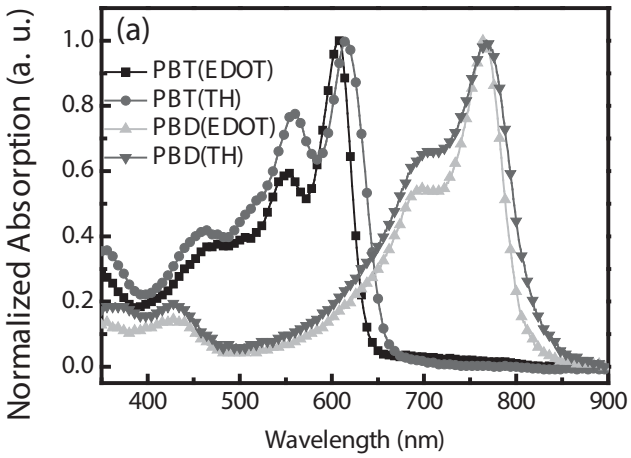

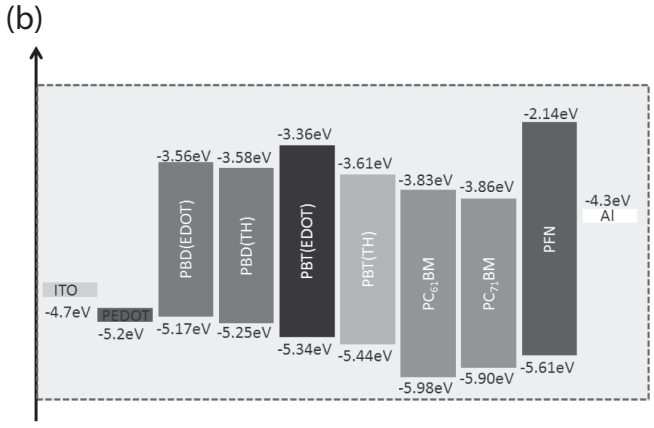

Figure 1. a) The film absorption spectra of the electron donor polymers; b) the energy levels of electron donors and acceptors measured by cyclic voltammetry. The energy levels of the interfacial layers and electrodes are also shown for reference.

2,7-(9,9-dioctylfluorene)] (PFN) modified Al as a cathode, and the photoactive layer of polymer/PCBM bulk heterojunction (≈100–140 nm) sandwiched between these two electrodes. It has been reported that the PFN layer could not only improve the electron extraction from the active layer to cathode, but also act as a hole blocking layer.[3,34] As a result, it could block the hole injection from the cathode, lowering the J_d at reverse bias.[35] The current–voltage characteristics of the polymer photodetectors are shown in **Figure 2**. Even with the presence of the PFN layer, the PBT(TH)-based photodetector still exhibited a relatively high J_d at reverse bias, which was as high as 10^{-5} A cm^{-2} at –2 V. Nevertheless, the J_d of PBT(EDOT) device was substantially lower than that of PBT(TH) device (Figure 2a). The PBT(EDOT) device exhibited a J_d of 5.9×10^{-9} A cm^{-2} at –2 V, more than three orders of magnitude lower than that of the PBT(TH) device. Such difference was also observed in the smaller bandgap DPP polymer system. The J_d of PBD(EDOT) device was around two orders of magnitude lower than that of PBD(TH) device at reverse bias (Figure 2b). The details of dark current densities at different biases were summarized in **Table 1**. At positive bias, both EDOT and thiophene functionalized polymers exhibited similar J_d after the injection barriers. The hole mobilities of these polymers were measured

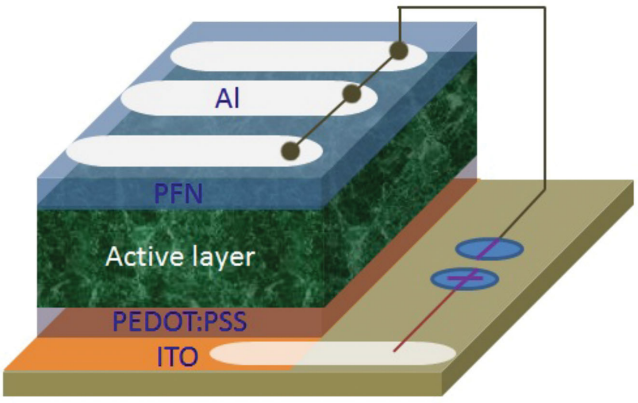

Scheme 2. The device structure of a polymer photodetector employed in this study.

by space-charge-limited current (SCLC) method (Supporting Information, Figure S4). The EDOT-based polymers exhibited just slightly lower mobilities than the thiophene-functionalized polymers, indicating that the introduction of EDOT unit does not significantly hinder charge transport. Thus, the rectification ratio of J_d at ±2.0 V for EDOT polymers was around 10^6–10^7, more than 100 times as high as thiophene polymers. The excellent diode characteristic observed from the EDOT-functionalized polymer devices indicates that the introduction

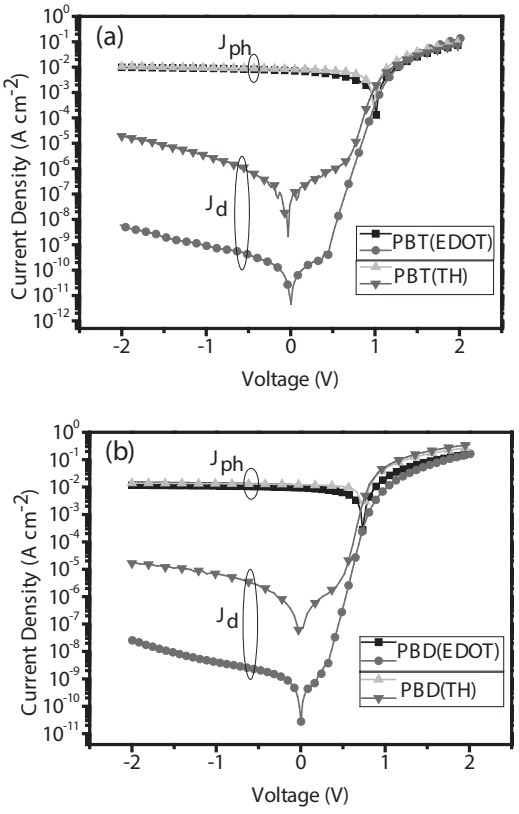

Figure 2. *J–V* characteristics of the polymer photodetectors in dark and under AM 1.5 G (100 mW cm^{-2}) illumination: a) PBT(EDOT) and PBT(TH) based photodetectors; b) PBD(EDOT) and PBD(TH) based photodetectors.

Table 1. The dark current J_d and photocurrent J_{ph} of polymer photodetectors with different electron donors.

Electron donor	Rectification ratio [at ±2V]	J_d (0 V) [A cm^{-2}]	J_d (–0.2 V) [A cm^{-2}]	J_d (–2V) [A cm^{-2}]	J_{ph} (0V)[a] [A cm^{-2}]
PBT(EDOT)	2.3×10^7	4.5×10^{-12}	1.6×10^{-10}	5.9×10^{-9}	7.22×10^{-3}
PBT(TH)	3.9×10^3	2.1×10^{-9}	2.2×10^{-7}	1.9×10^{-5}	8.39×10^{-3}
PBD(EDOT)	6.1×10^6	2.8×10^{-11}	8.8×10^{-10}	2.6×10^{-8}	1.02×10^{-2}
PBD(TH)	2.2×10^4	6.1×10^{-8}	8.1×10^{-7}	1.6×10^{-5}	1.21×10^{-2}
PBTI(EDOT)	2.4×10^6	3.5×10^{-10}	6.7×10^{-9}	1.1×10^{-7}	4.16×10^{-3}

[a]Measured under AM 1.5 G with a light intensity of 100 mW cm^{-2}.

of an EDOT unit in the side chain can significantly depress the intrinsic leakage current of the diode under dark conditions.

Under AM 1.5 G illumination, the photocurrent density (J_{ph}) of PBT(EDOT)/$PC_{61}BM$ device was comparable to that of PBT(TH) device, with a short-circuit current density of 7.22×10^{-3} A cm^{-2} for PBT(EDOT)/$PC_{61}BM$ device and 8.39×10^{-3} A cm^{-2} for PBT(TH)/$PC_{61}BM$ device, respectively (Figure 2a and Table 1). In the systems of DPP polymers with smaller bandgaps, both PBD(EDOT) and PBD(TH) devices also showed similar photocurrent densities (Figure 2b and Table 1). **Figure 3**a shows the EQEs of the polymer photodetectors measured at –0.2 V (the EQE spectra measured at other biases were provided in the Supporting Information, Figure S5). For TPD detectors, the PBT(EDOT) device showed almost the same

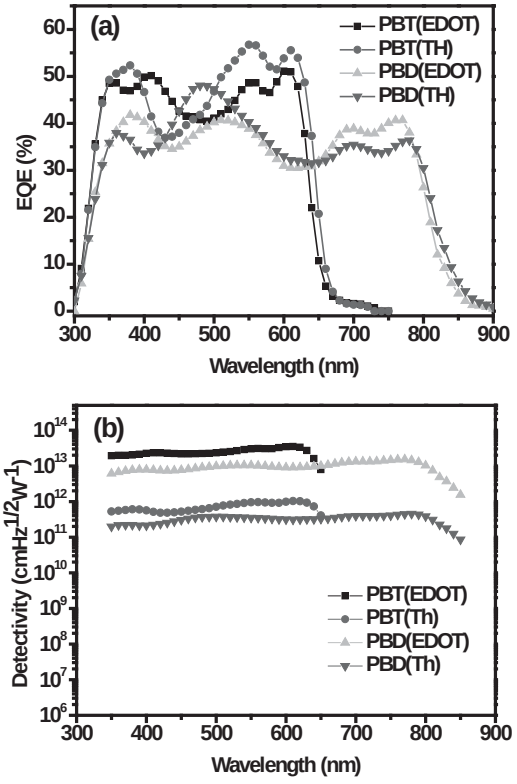

Figure 3. a) The external quantum efficiency (EQE) spectra and b) the detectivity of the polymer photodetectors aquired at –0.2 V bias.

EQE as PBT(TH) from 400 to 550 nm, just a slight blueshift of the maximum EQE compared with PBT(TH). For the smaller bandgap polymers, both PBD(EDOT) and PBD(TH) devices exhibited similar efficiency in converting photon to electron, with an average EQE of 40% from 400 to 800 nm, matching to their absorption spectra. This indicated that the introduction of EDOT did not affect the efficiency for charge carrier generation of the photodetector devices.

To calculate the detectivity (D^*) of photodetectors, we used the equation $D^* = \text{EQE} \times (\lambda/1240)/(2qJ_d)^{1/2}$, where q is the absolute charge of 1.60×10^{-19} C, J_d is the dark current density in A cm^{-2}, and λ is the wavelength in nm.[19] The detectivities of the polymer photodetectors at –0.2 V were shown in Figure 3b. For TPD polymers, the J_d of PBT(EDOT) device was 1.6×10^{-10} A cm^{-2} at –0.2 V in dark. As a result, PBT(EDOT) detector showed high detectivities of over 10^{13} Jones from 350 to 640 nm and a maximum detectivity of 3.5×10^{13} Jones at 610 nm. Nevertheless, PBT(TH) device showed detectivities of less than 1.1×10^{12} Jones within its response spectrum due to the relatively high J_d. For DPP polymers, the devices exhibited similar behaviors with TPD polymer detectors. In dark, the J_d of PBD(EDOT) device was 8.8×10^{-10} A cm^{-2} at –0.2 V. PBD(EDOT) device showed detectivities of over 6×10^{12} Jones from 400 to 810 nm, and achieved a peak detectivity of 1.5×10^{13} Jones at 770 nm, comparable to the best performance of inorganic photodetectors.[36] However, without the EDOT modification, PBD(TH) device showed a maximum detectivity of only 4.5×10^{11} Jones within the response spectrum. These results demonstrated that the introduction of EDOT side chains could afford efficient polymers for photodetector with high detectivities.

Noise current of the devices were analyzed and the noise spectra at various frequencies and dark currents are shown in **Figure 4**a,b, respectively. The noise current of the devices decreased as the modulation frequency increased. The EDOT-based devices exhibited low noise currents close to 2×10^{-14} A Hz$^{-1/2}$ at a modulation frequency of 100 Hz under –0.2 V bias, which approached to the shot noise limit. In contrast, the thiophene-based devices showed much larger noise currents of $>1 \times 10^{-12}$ A Hz$^{-1/2}$ at the same frequency. The low noise currents presented in the EDOT-based devices are favorable for small noise equivalent power (NEP)—the minimum input optical power that a detector can distinguish from noise. Using the equation NEP = i_n/R (i_n is the noise current in A, and R is the responsivity in A W^{-1}),[37,38] the NEP of the PBT(EDOT) and PBD(EDOT) detectors were calculated to be 7.2×10^{-14} W at 550 nm (–0.2 V, 100 Hz) and 1.1×10^{-13} W at 800 nm (–0.2 V, 100 Hz), respectively. This indicates that the PBT(EDOT) photodetector should be able to detect light intensity as low as 0.45 pW cm^{-2} at 550 nm, and PBD(EDOT) photodetector should be able to detect light intensity as low as 0.7 pW cm^{-2} at 800 nm. We employed a method recently reported by Huang and co-workers[39] to verify whether our polymer detectors could directly detect light intensity as low as NEP (Supporting Information). As shown in Figure 4c–f, the PBT(EDOT) and PBD(EDOT) photodetectors could response to the weak light linearly, and the lowest detectable light intensities were 0.48 pW cm^{-2} at 550 nm for PBT(EDOT) and 0.78 pW cm^{-2} at 800 nm for PBD(EDOT), respectively, which are very close to their calculated NEP values. Such small NEP

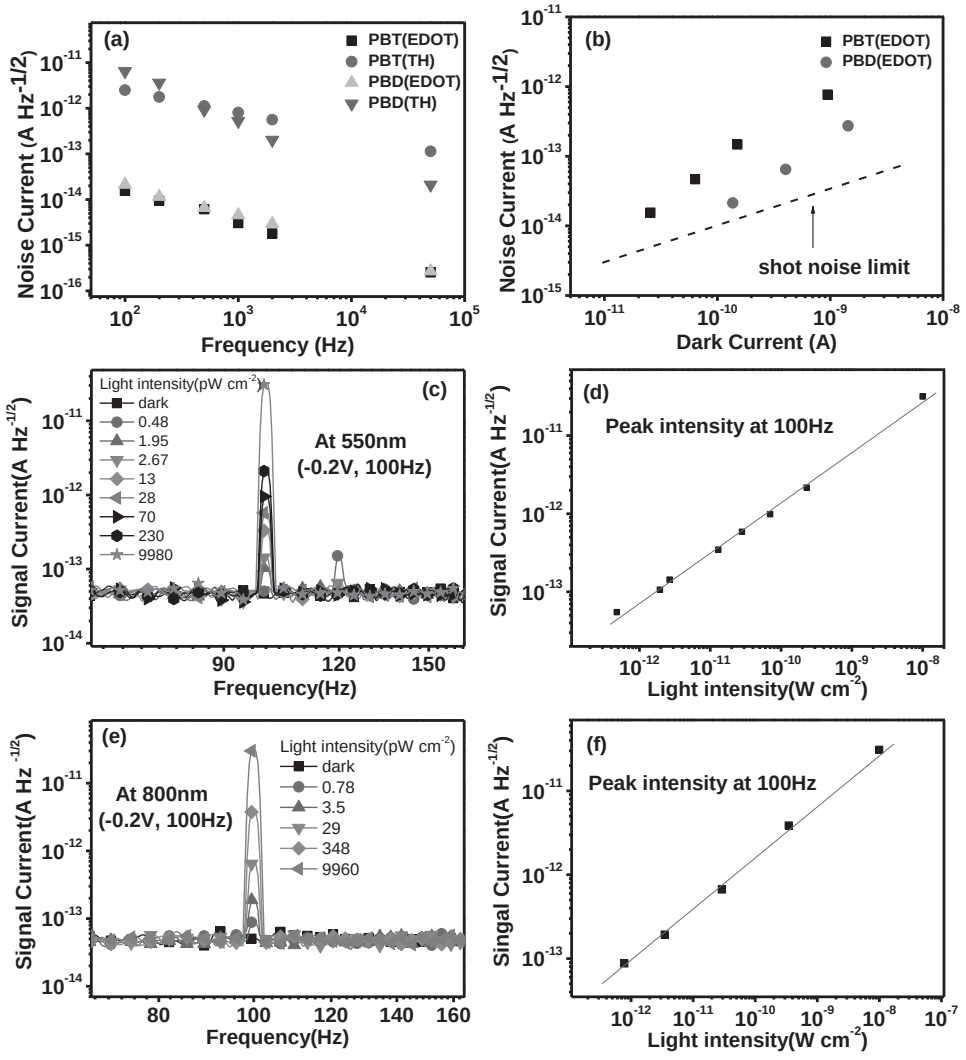

Figure 4. a) Noise current of the devices measured at different frequencies. b) Noise current as a function of dark current. The shot noise limit is also plotted for comparison. Direct NEP measurement of EDOT-polymer devices: c) The current spectra of PBT(EDOT) device at –0.2 V under 550 nm light illumination modulated at 100 Hz with different light intensities. d) The peak signal intensity at 100 Hz achieved from (c) as a function of light intensity. e) The current spectra of PBD(EDOT) device at –0.2 V under 800 nm light illumination modulated at 100 Hz with different light intensities. f) The peak signal intensity at 100 Hz achieved from (e) as a function of light intensity.

values indicated that the EDOT-functionalized polymers are good candidates for highly sensitive polymer photodetectors. In addition, our preliminary study showed that both the PBT(EDOT) and PBD(EDOT) photodetectors exhibited linear photoresponse under various green light (550 nm) intensities from nW cm^{-2} to mW cm^{-2}, suggesting a wide detecting range of our detectors (Supporting Information, Figure S6).

In bulk heterojunction system, it has been proposed that low dark current can be achieved by controlling the vertical phase segregation of electron donor/electron acceptor.[25] X-ray photoelectron spectroscopy (XPS) was employed to study the surface composition at the active layer/air interface after depositing the active layer on PEDOT substrate. As S atoms only present in the polymer, but not in PCBM, the S:C atomic ratio could unveil the distribution of polymer and PCBM in the active layer. The measured S:C atomic ratios for PBT(EDOT):$PC_{61}BM$ and PBT(TH):$PC_{61}BM$ blend films were 3.0% and 3.8%, respectively. Since the theoretical S:C atomic ratios (given polymer/$PC_{61}BM$ = 1/1, weight ratio) for them are 3.9% and 4.3%, respectively, this suggested that PCBM was enriched at the active layer/air interface in the PBT(EDOT) system to a greater extent than in the PBT(TH) system. To determine the composition distribution in the vertical direction, XPS depth profile of the TPD polymer:$PC_{61}BM$ blend films were used to probe the compostion from the air/active layer interface to the buried active layer/PEDOT/ITO interface (Supporting Information, Figure S7). PBT(EDOT):$PC_{61}BM$ blend film showed a remarkable S:C atomic ratio increase from 3.8% at etching time of 600 s to 11.8% at etching time of 800 s (this region was attributed to the interface between the active layer and the PEDOT:PSS layer), while the ratio in the PBT(TH):$PC_{61}BM$ film increased from 3.7% at etching time of 650 s to only 5.9% at etching time of 850 s. It indicated that polymers were enriched near the interface of active layer/PEDOT:PSS, and the higher S:C ratio in the

PBT(EDOT) system suggested that PBT(EDOT) exhibited a richer polymer content compared with PBT(TH). This gradation probably arose from the differences in surface energies between the EDOT polymers and thiophene-functionalized polymers, as well as the interaction with PEDOT:PSS. The surface tensions and spreading parameters (ΔW, defined as the capability of a droplet to attach to the substrate surface during spin-coating)[33,40] for the polymer and $PC_{71}BM$ solutions on PEDOT:PSS were measured (Supporting Information, Table S2). The magnitude of ΔW for EDOT-functionalized polymers is significantly smaller than thiophene-functionalized ones, suggesting that the EDOT units on the polymers could enhance the interaction between the polymer and the PEDOT layer. It caused the polymer accumulation at the active layer/PEDOT interface.[33] The polymer-rich layer at the active layer/PEDOT interface could block the electron injection from the anode, while the PCBM-rich layer could block the hole injection from the cathode.[41] These results demonstrated that the EDOT polymer systems exhibited favorable vertical phase separation, which could block the unfavorable charge injection at reverse bias. To further understand the effect of EDOT polymer, we deposited a thin layer of PBD(EDOT) on PEDOT/ITO substrate, then fabricated PBD(TH) photodetector device on it. With the PBD(EDOT) layer insertion, the PBD(TH) photodetector exhibited significantly lower dark current than the original PBD(TH) photodetector at reverse bias (Supporting Information, Figure S8). It suggested that the thin film of PBD(EDOT) layer might function as an electron blocking layer, which could block the electron injection from the anode at reverse bias. We conjecture that the favorable distribution of electron donor and acceptor and especially the polymer-rich layer on top of PEDOT in the EDOT polymer devices play an important role in reduciton of the dark current at reverse bias. By replacing the PEDOT:PSS layer with thermally evaporated molybdenum oxide (MoO_3) film, the EDOT-polymer-based photodetectors also showed good diode performance (Supporting Information, Figure S9). It suggested that the favorable vertical phase separation took place not only for the PEDOT substrates but also for molybdenum oxide substrates.

The surface characteristics of the active layer are also proposed to affect the magnitude of leakage current in the photodetectors.[42] As demonstrated by the tapping mode atomic force microscopy (AFM) measurement (Supporting Information, Figure S10), the active layers of both the EDOT and thiophene polymer devices exhibited smooth surface. The PBT(EDOT):$PC_{61}BM$ layer showed a root-mean-square (RMS) roughness of 1.89 nm in an area of 5 μm × 5 μm, smoother than the PBT(TH):$PC_{61}BM$ layer with an RMS roughness of 4.89 nm. The DPP-based polymer showed smaller difference, and the RMS roughnesses of PBD(EDOT):$PC_{71}BM$ and PBD(TH):$PC_{71}BM$ layers were 0.95 and 1.14 nm, respectively. The EDOT-based active layers with smoother surfaces could avoid the penetration of the top electrode into the active layer and afford a better contact with the top electrode, which may also contribute for the reduction of J_d.[24]

To further confirm the universality of the EDOT functionalization method, a low bandgap polymer PBTI(EDOT) containing EDOT-functionalized BDT as the donor unit and 4,4′-bis(alkyl)-[6,6′-bithieno[3,2-*b*]pyrrolylidene]-5,5′(4*H*,4′*H*)-dione (thienoisoindigo) as the acceptor unit was synthesized and used for the fabrication of polymer photodetectors (Supporting Information, Figure S11). PBTI(EDOT) exhibited a peak absorption at 840 nm and its absorption edge extended to 1085 nm (Supporting Information, Figure S11a). The optical bandgap of PBTI(EDOT) extracted from its absorption spectrum was about 1.14 eV. Figure S11b (Supporting Information) showed the current–voltage of its photodetector. The short-circuit current density observed from PBTI(EDOT) device was 4.16 mA cm^{-2} under AM 1.5 G illumination, possibly limited by the bulky side chains on the thienoisoindigo unit. Similar with the two EDOT-based polymers presented above, the PBTI(EDOT) device also exhibited good diode characteristics, with a rectification ratio of over 10^6 at ±2.0 V and a J_d of 6.7×10^{-9} A cm^{-2} at −0.2 V, indicating a low shot noise in the devices though PBTI(EDOT) had a bandgap as small as 1.14 eV. To determine the detectivity, the EQE was measured under −0.2 V bias (Supporting Information, Figure S11c) and the device responded from 400 to about 1085 nm, with two response peaks at 415 and 845 nm, respectively. The former peak showed an EQE of 30% and the latter was of 13%, indicating moderate photon-to-charge generation in the low bandgap polymer-based photodetectors. The detectivity of PBTI(EDOT) device exceeds 10^{12} Jones from 690 to 920 nm and is still over 10^{11} Jones even extending to 1040 nm. The highest detectivity approaches 1.8×10^{12} Jones at 830 nm, comparable to the results previously reported for low bandgap polymers.[24,43] All these results further demonstrated that the introduction of EDOT units could effectively depress the dark current of the devices and thus enhance the detectivity of photodetectors.

In conclusion, a molecular engineering method to prepare semiconducting polymers for photodetectors with enhanced detectivity is presented. Modified EDOT is employed as conjugated side chain to functionalize the backbone of the semiconducting polymers, which can significantly depress the dark current of the photodetectors but has little effect on charge transport and photovoltaic performance. It affords detectivity enhancement of more than one order of magnitude compared with thiophene-modified polymers. The introduction of EDOT unit increases the interaction between the polymer and the PEDOT layer, affording favorable vertical phase separation and forming polymer-rich layer near the PEDOT surface, which could account for the reduction of the dark current at reverse bias. With the active layer thickness of only 100–140 nm, the PBT(EDOT) and PBD(EDOT) photodetectors exhibited high rectification ratio (10^6–10^7) of dark current density at ±2.0 V and good photodetectivity of around 10^{13} Jones, and were capable to directly detect weak light down to 1 pW cm^{-2}. This approach could be applied to a variety of semiconducting polymers covering photoresponse range from UV to NIR, indicating its feasibility to construct advanced semiconducting polymers for efficient photodetectors.

Experimental Section

Materials: The synthesis of the conjugated polymers is available in the Supporting Information. [6,6]-Phenyl-C_{61}-butyric acid methyl

ester ($PC_{61}BM$, ≥99.5%) and [6,6]-phenyl-C_{71}-butyric acid methyl ester ($PC_{71}BM$, ≥99.5%) were obtained from American Dye Source, Inc. (Quebec, Canada). Chloroform (anhydrous, Aladdin) was purified by solvent purification system (Innovative Technology, Inc.) before device fabrication. 1,2-Dichlorobenzene (DCB, anhydrous) and 1,8-diiodoctance (DIO) were purchased from Sigma-Aldrich, Inc.

Fabrication of Polymer Photodetectors: The device structure was ITO/PEDOT:PSS/active layer/PFN/Al. The indium tin oxide (ITO) glass was sequential ultrasonic washed in acetone, detergent, deionized water, and isopropanol. Then the ITO substrate was dried in an oven and treated in an ultraviolet-ozone chamber for 4 min. Poly(3,4-ethylenedioxythiophene):poly(styrenesulfonate) (PEDOT:PSS, Clevios P VP AI4083) aqueous solution filtered through a 0.22 μm was spin-coated at 2500 rpm for 30 s on the ITO electrode, and then baked at 150 °C for 10 min in air. The thickness of the PEDOT:PSS layer was about 40 nm. Subsequently, the substrate was transferred to the nitrogen-filled glove box and the active layer was prepared. PBT(EDOT) and PBT(TH) were mixed with $PC_{61}BM$ (1:1, w/w) respectively and dissolved in chloroform/DIO (97:3, v/v). The thickness of these TPD films was about 100 nm. PBD(EDOT) and PBD(TH) were mixed with $PC_{71}BM$ (1:2, w/w) respectively and dissolved in chloroform/DCB (95:5, v/v). The thickness of these DPP films was about 130 nm. PBTI(EDOT) was blended with $PC_{71}BM$ (1:2, w/w) and dissolved in chloroform/DCB (95:5, v/v). The thickness of the PBTI(EDOT) film was about 100 nm. All the devices were covered with a poly[(9,9-bis(3′-(*N*,*N*-dimethylamino)propyl)-2,7-fluorene)-*alt*-2,7-(9,9-dioctylfluorene)] (PFN) layer before Al electrode deposition. Finally, the substrate was transferred to a vacuum chamber and a 100 nm of Al was thermally deposited on the active layer under a base pressure of 3×10^{-6} mbar. The photoactive area of the device was 0.16 cm^2.

Characterization of Polymer Photodetectors: The *J*–*V* measurement of the devices under AM 1.5 G solar simulator illumination (100 mW cm^{-2}) was performed on a computer-controlled Keithley 2400 Source Measure Unit in air. The *J*–*V* characteristics of the devices in dark were measured on a computer-controlled electrochemical workstation (Bio-Logic VSP). The EQE was measured under ambient atmosphere at room temperature using an Enlitech QE-R system. A bromine tungsten lamp was used as the light source. Noise current of the devices were measured by Enli Technology Co., Ltd. with a low noise current preamplifier (SR570, Stanford) and a lock-in amplifier. The current of the photodetectors for direct NEP measurement was recorded with the fast Fourier transform signal analyzer upon light input from a light-emitting diode (emission peak at 550 and 800 nm) modulated to be 100 Hz by a function generator.

Supporting Information

Supporting Information is available from the Wiley Online Library or from the author.

Acknowledgements

Y.Y.L. acknowledges the South University of Science and Technology of China for financial support and the funding from the "The Recruitment Program of Global Youth Experts of China." Y.Y.L. and T.B.Y. thank the Shenzhen fundamental research programs (No. JCYJ20130401144532128 and JCYJ20130401144532130) and "Peacock Plan" project (No. KQTD20140630110339343) for financial support. H.B.W. at SCUT thanks the National Nature Science Foundation of China (No. 51225301) for financial support. J.H. thanks the financial support from the Defense Threat Reduction Agency (Award No. HDTRA1–14–1–0030) for NEP measurement. L.Z.Z. and T.B.Y. contributed equally to this work.

Received: May 12, 2015
Revised: July 20, 2015
Published online: September 29, 2015

[1] P. Bujak, I. Kulszewicz-Bajer, M. Zagorska, V. Maurel, I. Wielgus, A. Pron, *Chem. Soc. Rev.* **2013**, *42*, 8895.
[2] T. K. Das, S. Prusty, *Polym.-Plast. Technol. Eng.* **2012**, *51*, 1487.
[3] G. Li, R. Zhu, Y. Yang, *Nat. Photon.* **2012**, *6*, 180.
[4] Y. Diao, L. Shaw, Z. Bao, S. C. B. Mannsfeld, *Energy Environ. Sci.* **2014**, *7*, 2145.
[5] R. R. Sondergaard, M. Hosel, F. C. Krebs, *J. Polym. Sci., Part B: Polym. Phys.* **2013**, *51*, 16.
[6] D. Tobjork, R. Osterbacka, *Adv. Mater.* **2011**, *23*, 1935.
[7] C. C. Chen, L. Dou, R. Zhu, C. H. Chung, T. B. Song, Y. B. Zheng, S. Hawks, G. Li, P. S. Weiss, Y. Yang, *ACS Nano.* **2012**, *6*, 7185.
[8] Y. Y. Liang, L. P. Yu, *Acc. Chem. Res.* **2010** , *43*, 1227.
[9] G. Yu, J. Gao, J. C. Hummelen, F. Wudl, A. J. Heeger, *Science* **1995**, *270*, 1789.
[10] T. B. Yang, M. Wang, C. H. Duan, X. W. Hu, L. Huang, J. B. Peng, F. Huang, X. Gong, *Energy Environ. Sci.* **2012**, *5*, 8208.
[11] H. Sirringhaus, P. J. Brown, P. J. Brown, M. M. Nielsen, K. Bechgaard, B. M. W. Langeveld-Voss, A. J. H. Spiering, R. A. J. Janssen, E. W. Meijer, P. Herwig, *Nature* **1999**, *401*, 685.
[12] H. Usta, A. Facchetti, T. J. Marks, *Acc. Chem. Res.* **2011**, *44*, 501.
[13] J. H. Burroughes, D. D. C. Bradley, A. R. Brown, R. N. Marks, K. Mackay, R. F. Friend, P. L. Burn, A. B. Holmes, *Nature.* **1990**, *347*, 539.
[14] M. A. Baldo, D. F. O'Brien, A. Shoustikow, S. Sibley, M. E. Thompson, S. R. Forrest, *Nature* **1998**, *395*, 151.
[15] G. Yu, K. Pakbaz, A. J. Heeger, *Appl. Phys. Lett.* **1994**, *64*, 3422.
[16] Y. Yao, Y. Y. Liang, V. Shrotriya, S. Q. Xiao, L. P. Yu, Y. Yang, *Adv. Mater.* **2007**, *19*, 3979.
[17] E. H. Sargent, *Adv. Mater.* **2008**, *20*, 3958.
[18] S. Kim, Y. T. Lim, E. G. Soltesz, A. M. De Grand, J. Lee, A. Nakayama, J. A. Parker, T. Mihaljevic, R. G. Laurence, D. M. Dor, L. H. Cohn, M. G. Bawendi, J. V. Frangioni, *Nat. Biotechnol.* **2004**, *22*, 93.
[19] X. Gong, M. Tong, Y. Xia, W. Cai, J. S. Moon, Y. Cao, G. Yu, C.-L. Shieh, B. Nilsson, A. J. Heeger, *Science* **2009**, *325*, 1665.
[20] X. Gong, M.-H. Tong, S. H. Park, M. Liu, A. Jen, A. J. Heeger, *Sensors* **2010**, *10*, 6488.
[21] P. Schilinsky, C. Waldauf, J. Hauch, C. J. Brabec, *Thin Solid Films* **2004**, *451–452*, 105.
[22] P. Schilinsky, C. Waldauf, C. J. Brabec, *Appl. Phys. Lett.* **2002**, *81*, 3885.
[23] Y. Xia, L. Wang, X. Deng, D. Li, X. Zhu, Y. Cao, *Appl. Phys. Lett.* **2006**, *89*, 081106.
[24] M. Kaltenbrunner, M. S. White, E. D. Glowacki, T. Sekitani, T. Someya, N. S. Sariciftci, S. Bauer, *Nat. Commun.* **2012**, *3*, 770.
[25] K.-J. Baeg, M. Binda, D. Natali, M. Caironi, Y.-Y. Noh, *Adv. Mater.* **2013**, *25*, 4267.
[26] E. Saracco, B. Bouthinon, J.-M. Verilhac, C. Celle, N. Chevalier, D. Mariolle, O. Dhez, J.-P. Simonato, *Adv. Mater.* **2013**, *25*, 6534.
[27] X. Liu, J. Zhou, J. Zheng, M. L. Becker, X. Gong, *Nanoscale* **2013**, *5*, 12474.
[28] X. Liu, H. Wang, T. Yang, W. Zhang, X. Gong, *ACS Appl. Mater. Interfaces* **2012**, *4*, 3701.
[29] X. Wang, H. Wang, W. Huang, J. Yu, *Org. Electron.* **2014**, *15*, 3000.
[30] L. Tong, C. Li, F. e. Chen, H. Bai, L. Zhao, G. Shi, *J. Phys. Chem. C* **2009**, *113*, 7411.
[31] J. H. Hou, M. H. Park, S. Q. Zhang, Y. Yao, L. M. Chen, J. H. Li, Y. Yang, *Macromolecules* **2008**, *41*, 6012.
[32] L. Dou, J. Gao, E. Richard, J. You, C.-C. Chen, K. C. Cha, Y. He, G. Li, Y. Yang, *J. Am. Chem. Soc.* **2012**, *134*, 10071.
[33] X. G. Guo, N. J. Zhou, S. J. Lou, J. Smith, D. B. Tice, J. W. Hennek, R. P. Ortiz, J. T. L. Navarrete, S. Y. Li, J. Strzalka, L. X. Chen, R. P. H. Chang, A. Facchetti, T. J. Marks, *Nat. Photonics* **2013**, *7*, 825.

[34] Z. He, C. Zhong, S. Su, M. Xu, H. Wu, Y. Cao, *Nat. Photonics* **2012**, *6*, 591.
[35] X. Hu, Y. Dong, F. Huang, X. Gong, Y. Cao, *J. Phys. Chem. C* **2013**, *117*, 6537.
[36] S. M. Sze, K. K. Ng, *Physics of Semiconductor Devices*, John Wiley & Sons, NJ, USA **2006**.
[37] L. Dou, Y. Yang, J. You, Z. Hong, W.-H. Chang, G. Li, Y. Yang, *Nat. Commun.* **2014**, *5*, 5404.
[38] G. Konstantatos, I. Howard, A. Fischer, S. Hoogland, J. Clifford, E. Klem, L. Levina, E. H. Sargent, *Nature* **2006**, *442*, 180.
[39] Y. Fang, J. Huang, *Adv. Mater.* **2015**, *27*, 2804.
[40] P. H. Wöbkenberg, J. Ball, F. B. Kooistra, J. C. Hummelen, D. M. de Leeuw, D. D. C. Bradley, T. D. Anthopoulos, *Appl. Phys. Lett.* **2008**, *93*, 013303.
[41] Z. Xiao, Y. Yuan, B. Yang, J. VanDerslice, J. Chen, O. Dyck, G. Duscher, J. Huang, *Adv. Mater.* **2014**, *26*, 3068.
[42] P. E. Keivanidis, P. K. H. Ho, R. H. Friend, N. C. Greenham, *Adv. Funct. Mater.* **2010**, *20*, 3895.
[43] G. Qian, J. Qi, Z. Y. Wang, *J. Mater. Chem.* **2012**, *22*, 12867.